



Special Feature: Novel Catalytic Approach

Research Report

A Study of the Gas Diffusion Mechanism in a Simulated Washcoat Layer Based on Experimentally Measured Effective Gas Diffusivity

Satoru Kato, Hironobu Ozeki, Hiroshi Yamada, Tomohiko Tagawa, Naoki Takahashi and Hirofumi Shinjoh

Report received on Feb. 2, 2016

■ABSTRACT■ The effective gas diffusivity affects the performance of automotive catalysts, so understanding gas diffusion phenomena in automotive catalysts is necessary in the design of automotive catalysts. We developed a method of directly measuring effective gas diffusivity, developed a measurement cell that can be used under heated conditions, and investigated the gas diffusion mechanism based on the Mean Transport Pore Model (MTPM). Effective gas diffusion coefficients were measured at 298 K, 473 K, and 673 K for nine gases: H₂, He, CH₄, Ne, N₂, O₂, C₃H₆, CO₂, and C₃H₈. Analysis based on the MTPM indicated that Knudsen and bulk diffusion take place simultaneously.

■KEYWORDS■ Catalyst, Diffusion, Porous Material, Pore Size Distribution, Washcoat Layer

1. Introduction

Typical catalytic reactors are sometimes operated in regions of significant diffusion limitation.⁽¹⁻¹⁰⁾ This limitation can be partially overcome by using monolithic catalysts coated in a catalyst layer on a honeycomb-type substrate. This is because the catalyst layer, which is known as a washcoat layer, can be as thin as 30-300 μm. Still, gas diffusion limitations affect the performance of monolithic catalysts.⁽¹¹⁻²⁰⁾

To design washcoat layers without diffusion limitations, evaluation methods that enable better understanding of diffusion phenomena are required. Methods for examining the effective diffusivity in the washcoat layer have been reported.⁽²¹⁻²⁴⁾ For example, Stary et al. measured the diffusivity of He and Ar through a washcoat layer using gas chromatography.⁽²³⁾ Zhang et al. measured the diffusivity of CO through a washcoat layer with a modified Wicke-Kallenbach-type diffusion cell.⁽²⁴⁾ These conventional studies had two disadvantages. The first is that these methods sometimes estimate an invalid effective diffusivity. Because the washcoat layer cannot be separated from the cordierite substrate, the gas diffusivity through the washcoat layer must be obtained by deducting the gas diffusivity of the substrate. This sometimes leads to an invalid result. The other problem is that diffusivity was not measured

at actual operating temperatures. When an automotive catalytic converter is employed in the Federal Test Procedure, the catalyst temperature is in the range of 300 to 1073 K.⁽²⁵⁾ However, the effective diffusivity is measured at 298 K in the conventional method.⁽²¹⁻²⁴⁾

To solve these problems, we developed a method of directly measuring the effective gas diffusivity,⁽²⁶⁾ and also developed a measurement cell that can be used under heated conditions.⁽²⁷⁾ In this paper, we report on recent developments^(26,27) and discuss a gas diffusion mechanism based on our latest data⁽²⁸⁾ and the Mean Transport Pore Model (MTPM).⁽²⁹⁾

2. Experimental

2.1 Development of Simulated Washcoat Layer to Directly Measure Effective Gas Diffusivity

We used a “simulated washcoat layer” to avoid one problem with the conventional method; the gas diffusivity in the cordierite substrate makes it difficult to evaluate the gas diffusivity in the washcoat layer.⁽²⁶⁾ A metal mesh substrate was used instead of a cordierite substrate, making it possible to evaluate the gas diffusivity directly because the metal mesh has no diffusion resistance. The procedure used to prepare the sample is described below.

The simulated washcoat layer used in the experiments

was made from ZrO_2 , which was applied to a metal mesh by dipping it into slurry containing ZrO_2 powder and zirconium nitrate. The metal mesh was made of stainless steel. The samples obtained were dried at 393 K for 12 hours and then calcined at 773 K for 1 hour.⁽²⁶⁾

2.2 Development of Wicke-Kallenbach-type Diffusion Cell for Use under Heated Conditions

The Wicke-Kallenbach-type diffusion cell that we developed was made from SUS304, and used a metal O-ring, enabling measurements under heated conditions.⁽²⁷⁾ Previously reported Wicke-Kallenbach-type cells were not used under heated conditions.^(21,22,24) This is because the conventional diffusion cell uses epoxy resin and/or rubber O-rings, which prevent gas from leaking from the diffusion cell, and these materials cannot be used under heated conditions. **Figure 1(a)** shows a cross-sectional view of the cell developed in our previous research.⁽²⁷⁾ A photograph of the cell is shown in Fig. 1(b).

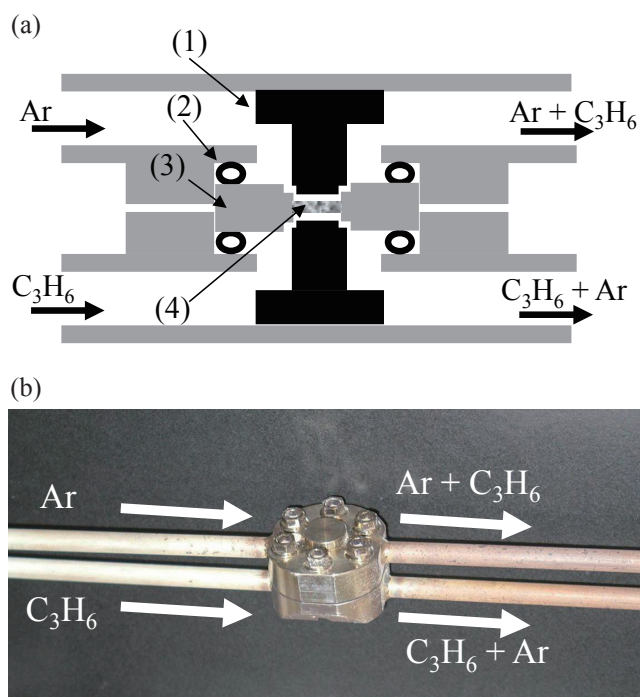


Fig. 1 (a) The Wicke-Kallenbach-type counter-current diffusion cell: (1) gas current control section, (2) metal O-ring, (3) SUS section to fix to metal mesh, and (4) simulated washcoat layer. (b) Photograph of the diffusion cell.

2.3 Evaluating Gas Diffusivity

As shown in Fig. 1(a), a simulated washcoat layer separated the upper and lower compartments. The gas being evaluated, such as C_3H_6 , was fed into the lower compartment. The paired gas that was used along with the evaluated gas was Ar. Ar was suitable for use with a thermal conductivity detector (TCD). Although Ar is not present when an automotive catalyst is employed, the main purpose of this research was to investigate the gas diffusion phenomena. The effective diffusion coefficient was calculated from the gas concentration in the outlet flow. Recently, we measured the effective diffusion coefficient for H_2 , He, CH_4 , Ne, N_2 , O_2 , C_3H_6 , CO_2 , and C_3H_8 at 298 K, 473 K, and 673 K.⁽²⁸⁾

3. Results & Discussion

First, the temperature and gas species dependence of the effective diffusivity⁽²⁸⁾ is reported. Next, an analysis based on MTPM is described. Finally, the gas diffusion mechanism in the simulated washcoat layer is discussed.

3.1 Temperature and Gas Species Dependence of Effective Diffusivity

The relationship between effective diffusion coefficient and molecular weight is shown in **Fig. 2**. The driving force for the gas diffusion phenomena was the random motion of the gas molecules. The mean molecular speed is given by Eq. (1), in which R , T , and M are the gas constant, temperature, and molecular weight, respectively. The increase in effective diffusion

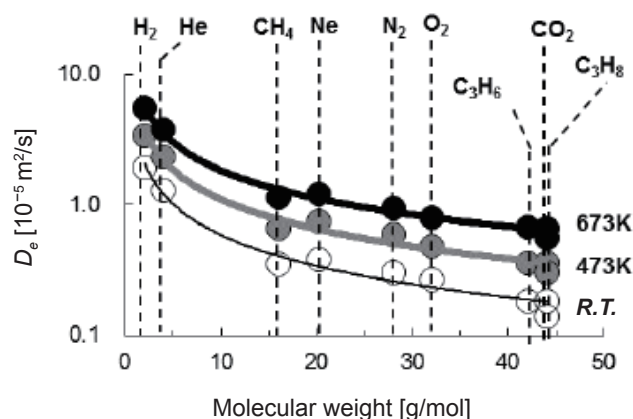


Fig. 2 Temperature and gas species dependence of effective diffusivity.

coefficient with increasing temperature or decreasing molecular weight is due to an increase in the mean molecular speed. This is reasonable.

$$v_m = \left(\frac{8RT}{\pi M} \right)^{1/2} \quad (1)$$

3.2 Analysis Based on Mean Transport Pore Model

We previously reported that bulk and Knudsen diffusion took place simultaneously within a simulated washcoat layer.⁽²⁷⁾ Hence, effective gas diffusion coefficients ($D_{eff,ij}$) in a binary gas diffusion system (diffusion of gas species i in gas species j) can be described as in Eq. (2), which is a modified Stefan-Maxwell equation (see e.g. Ref. (29)). Here, $D_{eff,i}^k$, $D_{eff,ij}^b$, α_i , and y_i are the effective Knudsen diffusion coefficient, the effective bulk diffusion coefficient, a correction term for differences in the molecular weights of the gas species, and the molar fraction, respectively. In this paper, MTPM⁽²⁹⁾ was used to analyze the experimental data. This model can provide information regarding pore structure. MTPM describes $D_{eff,ij}^b$ and $D_{eff,i}^k$ as Eq. (3a) and Eq. (3b).⁽²⁹⁾

$$\left(1/D_{eff,ij} \right) = \left(1/D_{eff,i}^k \right) + (1 - \alpha_i y_i) / D_{eff,ij}^b \quad (2)$$

$$\alpha_i = 1 - (M_i/M_j)^{1/2} \quad (2a)$$

$$D_{eff,ij}^b = \psi D_{ij}^b \quad (3a)$$

$$D_{eff,i}^k = r\psi K_i \quad (3b)$$

Here, D_{ij}^b and K_i are bulk diffusion coefficients and Knudsen coefficients, respectively, and ψ and r represent the geometric factor and the mean diffuse pore radius in MTPM. An important point of MTPM is that ψ and r are estimated from experimentally measured effective diffusion coefficients. The procedure is described as follows.

Eq. (4) is obtained by substituting Eq. (3a) and Eq. (3b) into Eq. (2).

$$\left(1/D_{eff,ij} \right) = \left(1/r\psi K_i \right) + (1 - \alpha_i y_i) / (\psi D_{ij}^b) \quad (4)$$

Eq. (4) is converted to Eq. (5).

$$\left(K_i/D_{eff,ij} \right) = \left(1/r\psi \right) + (1/\psi) \{ (1 - \alpha_i y_i) K_i/D_{ij}^b \} \quad (5)$$

Then, the effective diffusion coefficient shown in Fig. 2, the molar fraction, the bulk diffusion coefficient, and the Knudsen diffusion coefficient were substituted into Eq. (5), with the results shown in Fig. 3. Almost all of the data points fall on a straight line. This means that the data set used in the present research can be analyzed with MTPM.

The intercept and slope of the straight line in Fig. 3 provide the mean transport parameters r (362 nm) and ψ (0.16). The values of r and ψ represent structural property of porous material. For example, Schneider et al. reported that the r and ψ values of form of catalyst pellets were 340 nm and 0.017, respectively.⁽²⁹⁾ The large difference in ψ between the reported value (0.017) and the value obtained in the present research (0.16) may be due to some difference in the pore structure, such as the porosity.

3.3 Contribution of Knudsen Diffusion to Net Diffusion

The first step of the catalytic reaction is the adsorption of gas molecules onto active sites on the pore wall in the washcoat layer. Since collisions between the pore walls and gas molecules are classified as Knudsen diffusion, we believe that controlling Knudsen diffusion is one solution to avoid diffusional limitations on catalytic performance. Knudsen diffusion can be controlled by modifying the pore structure, but this requires understanding the contribution of Knudsen diffusion to net diffusion, which can be understood as the percentage value of Knudsen diffusion. The calculation procedure was as follows.

Since diffusion resistance is the inverse of the diffusion coefficient, Eq. (2) means that the total

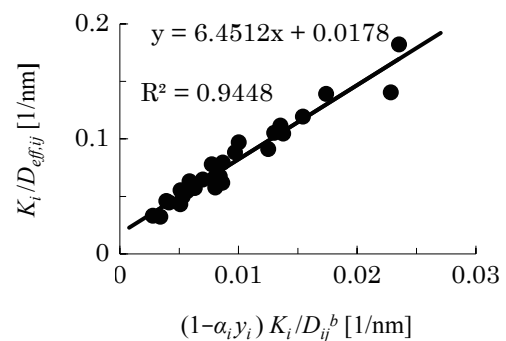


Fig. 3 Plot of $(1 - \alpha_i y_i) K_i / D_{ij}^b$ vs $K_i / D_{eff,ij}$.

diffusion resistance can be explained as the sum of the Knudsen diffusion resistance and the bulk diffusion resistance. Hence, the contribution of Knudsen diffusion to net diffusion can be calculated as a percentage value of Knudsen diffusion. As shown in Fig. 4, the percentage value of Knudsen diffusion varied widely by gas species and was also dependent on temperature. For example, at 298 K, the minimum value was 12% for C_3H_8 , and the maximum value was 33% for He. At 673 K, the minimum value was 30% for C_3H_8 , and the maximum value was 56% for He. Starýa et al. reported on gas diffusivity in a washcoat layer on a cordierite substrate for Ar/ N_2 pairs,⁽²³⁾ and determined that the contribution of Knudsen diffusion to net diffusion was 36% at 298 K. On the other hand, in this research, a value of 21% for N_2 at 298 K was obtained. The difference may be due to a difference in pore structure.

The conventional capillary tube model describes how pore size and λ_A affect the gas diffusion mechanism. In the conventional capillary tube model, the gas diffusion mechanism depends on r_e/λ_A , where r_e is the inner radius of the capillary tube.⁽³⁰⁾ When r_e/λ_A is less than 0.1, the Knudsen diffusion mechanism is dominant, whereas the bulk diffusion mechanism is dominant when r_e/λ_A is over 10. When r_e/λ_A is between 0.1 and 10, the gas diffusion mechanism is in a transition region between bulk and Knudsen diffusion. Since the pore structure of the simulated washcoat layer is complex, it is difficult to determine

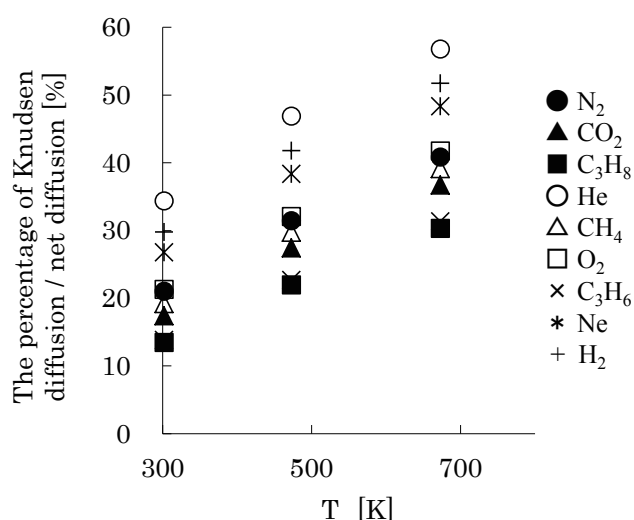


Fig. 4 Temperature dependence of the proportion of Knudsen transport.

a pore size in order to predict the diffusion mechanism. Here, we focus on the mean diffusive radius (r). Using r instead of r_e , the resulting relationship between r/λ_A and the percentage of Knudsen diffusion is shown in Fig. 5. When r/λ_A was between 1 and 8, the proportion of Knudsen diffusion was between 60% and 10%. This relationship is in accordance with the conventional capillary tube model. Although the pore structure of the simulated washcoat layer was complex, and there were pore size and tortuosity distributions, Fig. 5 indicates that r is in accordance with r_e in the conventional capillary tube model. In other words, the complex pore structure of the simulated washcoat layer can be consistently simplified by using the MTPM.

Either temperature or gas species dependence of the Knudsen diffusion on total diffusion, as shown in Fig. 4, indicates that the optimal pore size depends on gas species and catalytic reaction. To fully explain what size of pore is effective for catalytic performance, we intend to perform a more detailed investigation of the relationship between the Knudsen diffusion contribution and catalytic performance as future work.

4. Conclusion

To better understand gas diffusion phenomena in the washcoat layer, we developed a method of directly measuring effective gas diffusivity, and also developed a measurement cell that can be used under heated conditions. The data set of effective diffusion

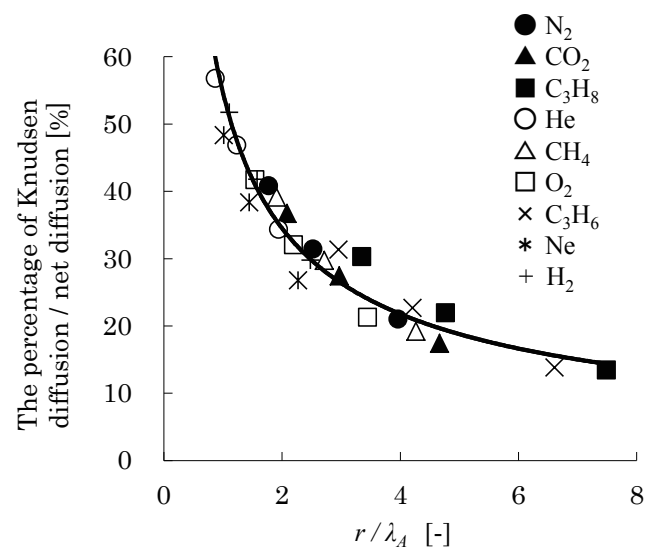


Fig. 5 Relationship between the proportion of Knudsen transport and r/λ_A .

coefficients was measured in a binary gas diffusion system using a modified Wicke-Kallenbach diffusion cell at 298 K, 473 K, and 673 K. H₂, He, CH₄, Ne, N₂, O₂, C₃H₆, CO₂, and C₃H₈ gases were investigated, with Ar as a paired gas in the measurements. The experimentally measured effective diffusivity data were successfully analyzed using the MTPM. The mean diffuse pore radius and geometric factor were 362 nm and 0.16. The percentage contribution of Knudsen diffusion to total diffusion varied widely with gas species and depended on temperature. At 298 K, the minimum value was 12% for C₃H₈, and the maximum value was 33% for He. At 673 K, the minimum value was 30% for C₃H₈, and the maximum value was 56% for He. Either temperature or gas species dependence of the Knudsen diffusion on total diffusion can be explained with the ratio of mean diffusive pore radius and mean free path. When r/λ_A was between 1 and 8, the proportion of Knudsen diffusion was between 60% and 10%. This relationship was in accordance with the conventional capillary tube model, indicating that the complex pore structure of the simulated washcoat layer can be simplified by using the MTPM. Investigation of the relationship between the contribution of Knudsen diffusion and the catalytic performance will be performed as future work.

Acknowledgement

We thank Mr. Itoh of Nagoya University for his helpful comments in the view point of diffusion cell.

Nomenclature

$D_{eff,i}$	effective diffusion coefficient of gas species i , m ² /s
$D_{eff,i}^k$	effective Knudsen diffusion coefficients of gas species i , m/s
$D_{eff,ij}^b$	effective binary bulk diffusion coefficient of the pair i - j , m ² /s
D_{ij}^b	binary bulk diffusion coefficient of the pair i - j , m ² /s
K_i	Knudsen diffusion constant of gas species i , m/s
r	mean diffusive pore radius, m
r_e	capillary radius
y_i	molar fraction of component i
Ψ	ratio of diffusive pore porosity and tortuosity

Reference

- (1) Visconti, C. G., Tronconi, E., Lietti, L., Groppi, G., Forzatti, P., Cristiani, C., Zennaro, R. and Rossini, S., "An Experimental Investigation of Fischer-Tropsch Synthesis over Washcoated Metallic Structured Supports", *Appl. Catal. A*, Vol. 370, No. 1-2 (2009), pp. 93-101.
- (2) Sie, S. T. and Krishna, R., "Fundamentals and Selection of Advanced Fischer-Tropsch Reactors", *Appl. Catal. A*, Vol. 186, No. 1-2 (1999), pp. 55-70.
- (3) Enger, B. C., Lodeng, R., Holmen, A., "Evaluation of Reactor and Catalyst Performance in Methane Partial Oxidation over Modified Nickel Catalysts", *Appl. Catal. A*, Vol. 364, No. 1-2 (2009), pp. 15-26.
- (4) Enger, B. C., Lodeng, R. and Holmen, A., "A Review of Catalytic Partial Oxidation of Methane to Synthesis Gas with Emphasis on Reaction Mechanisms over Transition Metal Catalysts", *Appl. Catal. A*, Vol. 346, No. 1-2 (2008), pp. 1-27.
- (5) Łojewska, J., Kołodziej, A., Łojewski, T., Kapica, R. and Tyczkowski, J., "Structured Cobalt Oxide Catalyst for VOC Combustion. Part I: Catalytic and Engineering Correlations", *Appl. Catal. A*, Vol. 366, No. 1 (2009), pp. 206-211.
- (6) Solsvik, J. and Jakobsen, H. A., "A Survey of Multicomponent Mass Diffusion Flux Closures for Porous Pellets: Mass and Molar Forms", *Transp. Porous. Media*, Vol. 93 (2012), pp. 99-126.
- (7) Tiemersma, T. P., Chaudhari, A. S., Gallucci, F., Kuipers, J. A. M. and van Sint Annaland, M., "Integrated Autothermal Oxidative Coupling and Steam Reforming of Methane. Part 1: Design of a Dual-function Catalyst Particle", *Chem. Eng. Sci.*, Vol. 82 (2012), pp. 200-214.
- (8) Solsvik, J. and Jakobsen, H. A., "Modeling of Multicomponent Mass Diffusion in Porous Spherical Pellets: Application to Steam Methane Reforming and Methanol Synthesis", *Chem. Eng. Sci.*, Vol. 66, No. 9 (2011), pp. 1986-2000.
- (9) Lualdi, M., Lögdberg, S., Di Carlo, G., Järås, S., Boutonnet, M., Venezia, A. M., Blekkan, E. A. and Holmen, A., "Evidence for Diffusion-controlled Hydrocarbon Selectivities in the Fischer-Tropsch Synthesis over Cobalt Supported on Ordered Mesoporous Silica", *Top. Catal.*, Vol. 54 (2011), pp. 1175-1184.
- (10) Weber, D., Holland, D. J. and Gladden, L. F., "Spatially and Chemically Resolved Measurement of Intra- and Inter-particle Molecular Diffusion in a Fixed-bed Reactor", *Appl. Catal. A*, Vol. 392, No. 1 (2011), pp. 192-198.
- (11) Leung, D., Hayes, R. E. and Kolaczkowski, S. T., "Diffusion Limitation Effects in the Washcoat of a Catalytic Monolith Reactor", *Can. J. Chem. Eng.*, Vol. 74, No. 1 (1996), pp. 94-103.
- (12) Hayes, R. E. and Kolaczkowski, S. T., "Mass and

- Heat Transfer Effects in Catalytic Monolith Reactors”, *Chem. Eng. Sci.*, Vol. 49, No. 21 (1994), pp. 3587-3599.
- (13) Kočí, P., Kubiček, M. and Marek, M., “Modelling of TWC Monolith Converters with Microkinetics and Diffusion in the Washcoat”, *Ind. Eng. Chem. Res.*, Vol. 43, No. 16 (2004), pp. 4503-4510.
- (14) West, D. H., Balakotaiah, V. and Jovanovic, Z., “Experimental and Theoretical Investigation of the Mass Transfer Controlled Regime in Catalytic Monoliths”, *Catal. Today*, Vol. 88, No. 1-2 (2003), pp. 3-16.
- (15) Mukadi, L. S. and Hayes, R. E., “Modelling the Three-way Catalytic Converter with Mechanistic Kinetics Using the Newton–Krylov Method on a Parallel Computer”, *Comput. Chem. Eng.*, Vol. 26, No. 3 (2002), pp. 439-455.
- (16) Ramanathan, K., Balakotaiah, V. and West, D. H., “Light-off Criterion and Transient Analysis of Catalytic Monoliths”, *Chem. Eng. Sci.*, Vol. 58, No. 8 (2003), pp. 1381-1405.
- (17) Nova, I., Bounechada, D., Maestri, R. and Tronconi, E., “Influence of the Substrate Properties on the Performances of NH₃-SCR Monolithic Catalysts for the Aftertreatment of Diesel Exhaust: An Experimental and Modeling Study”, *Ind. Eng. Chem. Res.*, Vol. 50, No. 1 (2011), pp. 299-309.
- (18) Novák, V., Kóčí, P., Marek, M., Štěpánek, F., Blanco-García, P. and Jones, G., “Multi-scale Modelling and Measurements of Diffusion through Porous Catalytic Coatings: An Application to Exhaust Gas Oxidation”, *Catal. Today*, Vol. 188, No. 1 (2012), pp. 62-69.
- (19) Kota, A. S., Luss, D. and Balakotaiah, V., “Micro-kinetics of NO_x Storage and Reduction with H₂/CO/C₃H₆ on Pt/BaO/Al₂O₃ Monolith Catalysts”, *Chem. Eng. J.*, Vol. 262 (2015), pp. 541-551.
- (20) Shakya, B. M., Harold, M. P. and Balakotaiah, V., “Simulations and Optimization of Combined Fe- and Cu-zeolite SCR Monolith Catalysts”, *Chem. Eng. J.*, Vol. 278 (2015), pp. 374-384.
- (21) Beeckman, J. W., “Measurement of the Effective Diffusion Coefficient of Nitrogen Monoxide through Porous Monolith-type Ceramic Catalysts”, *Ind. Eng. Chem. Res.*, Vol. 30, No. 2 (1991), pp. 428-430.
- (22) Hayes, R. E., Kolaczowski, S. T., Li, P. K. C. and Awdry, S., “Evaluating the Effective Diffusivity of Methane in the Washcoat of a Honeycomb Monolith”, *Appl. Catal. B*, Vol. 25, No. 2-3 (2000), pp. 93-104.
- (23) Sary, T., Šolcová, O., Schneider, P. and Marek, M., “Effective Diffusivities and Pore-transport Characteristics of Washcoated Ceramic Monolith for Automotive Catalytic Converter”, *Chem. Eng. Sci.*, Vol. 61, No. 18 (2006), pp. 5934-5943.
- (24) Zhang, F., Hayes, R. E. and Kolaczowski, S. T., “A New Technique to Measure the Effective Diffusivity in a Catalytic Monolith Washcoat”, *Chem. Eng. Res. Des.*, Vol. 82, No. 4 (2004), pp. 481-489.
- (25) Yamauchi, T., Kubo, S., Mizukami, T., Sato, N. and Aono, N., “Numerical Simulation for Designing Next Generation TWC System with Detailed Chemistry”, *SAE Tech. Paper Ser.*, 2008-01-1540 (2008).
- (26) Kato, S., Ozeki, H., Yamada, H., Tagawa, T., Takahashi, N. and Shinjoh, H., “Direct Measurements of Gas Diffusivity in a Washcoat Layer under Steady State Conditions at Ambient Temperature”, *J. Ind. Eng. Chem.*, Vol. 19, No. 3 (2013), pp. 835-840.
- (27) Kato, S., Ozeki, H., Yamada, H., Tagawa, T., Takahashi, N. and Shinjoh, H., “Direct Measurements of Gas Diffusivity in a Washcoat Layer under Steady State and Heated Conditions”, *Chem. Eng. J.*, Vol. 271 (2015), pp. 188-194.
- (28) Kato, S., Ozeki, H., Yamada, H., Tagawa, T., Takahashi, N. and Shinjoh, H., “Analysis of the Gas Diffusivity in the Simulated Washcoat Layer Based on Mean Transport Pore Model and the Mean Molecular Speed”, *Chem. Eng. Trans.*, Vol. 43 (2015), pp. 1591-1596.
- (29) Schneider, P. and Gelbin, D., “Direct Transport Parameters Measurement Versus Their Estimation from Mercury Penetration in Porous Solids”, *Chem. Eng. Sci.*, Vol. 40, No. 7 (1985), pp. 1093-1099.
- (30) Hill, C. G., *An Introduction to Chemical Engineering Kinetics & Reactor Design* (1981), pp. 433-435, John Wiley & Sons, Inc.

Fig. 1

Reprinted from *Chem. Eng. J.*, Vol. 271 (2015), pp. 188-194, Kato, S., Ozeki, H., Yamada, H., Tagawa, T., Takahashi, N. and Shinjoh, H., Direct Measurements of Gas Diffusivity in a Washcoat Layer under Steady State and Heated Conditions, © 2015 Elsevier B. V., with permission from Elsevier.

Fig. 2

Reprinted from *Chem. Eng. Trans.*, Vol. 43 (2015), pp. 1591-1596, Kato, S., Ozeki, H., Yamada, H., Tagawa, T., Takahashi, N. and Shinjoh, H., Analysis of the Gas Diffusivity in the Simulated Washcoat Layer Based on Mean Transport Pore Model and the Mean Molecular Speed, © 2015 AIDIC Servizi S.r.l., with permission from AIDIC.

Satoru Kato

Research Field:

- Catalyst and Catalysis

Academic Societies:

- Catalysis Society of Japan
- The Society of Chemical Engineers, Japan

**Hirofumi Shinjoh**

Research Field:

- Catalyst and Catalysis

Academic Degree: Dr.Eng.

Academic Societies:

- Catalysis Society of Japan
- The Society of Chemical Engineers, Japan
- The Chemical Society of Japan

Awards:

- Award of New Technology, The Japan Society of Mechanical Engineers, 1995
- Award of Chemical Technology, The Chemical Society of Japan, 2009

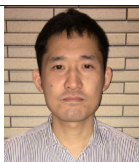
**Hironobu Ozeki***

Research Fields:

- Chemical Reaction Engineering
- Catalysis

Academic Society:

- The Society of Chemical Engineers, Japan



* Nagoya University

Hiroshi Yamada*

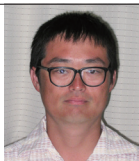
Research Field:

- Chemical Reaction Engineering

Academic Degree: Dr.Eng.

Academic Societies:

- The Society of Chemical Engineers, Japan
- The Japan Petroleum Institute
- Catalysis Society of Japan
- The Society of Eco-Engineering

**Tomohiko Tagawa***

Research Fields:

- Chemical Reaction Engineering
- Catalysis

Academic Degree: Dr.Eng.

Academic Societies:

- The Society of Chemical Engineers, Japan
- The Chemical Society of Japan
- The Japan Petroleum Institute
- Catalysis Society of Japan

**Naoki Takahashi**

Research Field:

- Catalyst and Catalysis

Academic Degree: Dr.Eng.

Academic Societies:

- Catalysis Society of Japan
- Society of Automotive Engineers of Japan
- The Ceramic Society of Japan

Awards:

- Outstanding Poster Presentation Award, Catalysis Society of Japan, 2008 and 2013

